

# Short Note: Generating regional permeability maps for large-scale hydrogeological studies

D.K. Khan (dkkhan@ualberta.ca)  
Department of Earth & Atmospheric Sciences  
University of Alberta

## Abstract

*This short note summarizes the results of a term project by the author for a course in geostatistical applications. A practical geostatistical methodology enables the hydrogeologist to add spatial permeability distributions to the set of maps generated in a regional hydrogeological mapping project. A case study is presented outlining the steps in a suggested geostatistical methodology including: 1) variogram modeling, 2) kriging and cross-validation of the probability model, 3) scaling of the variogram model and data histogram to correct for the discrepancy between the simulation scale and the scale of the data, and 4) Sequential Gaussian Simulation to generate realizations of the permeability field conditional to the measured data. The geostatistical method treats the problem in a probabilistic framework; therefore it does not provide a single best rendering of the distribution of permeability, but some relatively simple post-processing steps may enable selection of a small number of representative permeability maps from a large set of equally probable realizations. A deemed-representative model of regional permeability enables direct estimates of variable groundwater flux over an area.*

## Introduction

Hydrogeological mapping of sedimentary basins reveals large-scale features in aquifer potentiometric surfaces directly related to regional permeability variation [10]. Understanding the interplay between rock permeability and associated phenomena such as anomalous pressures and migration and accumulation of petroleum is relevant to basin analysis and petroleum exploration. In regional aquifer studies, formation pressures and water chemistry from drill stem tests are mapped to understand present-day and paleo-hydrogeological factors influencing petroleum occurrence [2,5].

Formation water flow can be inferred from the gradient of hydraulic head where a map of an aquifer's potentiometric surface can be produced from sufficient data. Recent petroleum hydrogeological studies have pioneered the mapping of fluid driving force directions accounting for the combined effect of hydraulic gradients, water density gradients and geologic structure [1]. Darcy's Law relates fluid driving force to flow rate such that a spatial distribution of permeability combined with a map of fluid driving forces in an aquifer allows estimation of spatially variable fluid fluxes. Distributions of groundwater fluxes are important to risk analysis in subsurface disposal operations such as geologic CO<sub>2</sub> sequestration. The following case study outlines a practical methodology for generating representative spatial distributions of permeability from drill-stem test data to complement regional hydrogeological mapping thereby helping to port the maps to the next level of analysis, such as a numerical modeling study, in a self-consistent manner.

## Case Study: Birdbear Aquifer, Williston Basin - SE Saskatchewan, and West-Central U.S.A.

The Birdbear Formation is a regionally extensive Devonian-age carbonate aquifer with numerous Drill Stem Tests (DST's) from petroleum exploration wells that provide good data coverage in the study area (Figure 1). A potentiometric surface map constructed from these data represents the present-day steady-state groundwater flow field, after removing data points affected by pressure drawdown from petroleum production. The potentiometric surface map shows the distribution of hydraulic head and the gradient of head, which varies over the map as a result of heterogeneity in aquifer permeability (Figure 2). An average intrinsic permeability over the packed-off zone of each DST can be calculated by a Horner straight-line extrapolation from the slope of the pressure build-up curve and an average flow rate of a single fluid. This permeability is taken as an average effective permeability of the rock volume within which the pore-pressure disturbance propagates during the flow period of the DST.

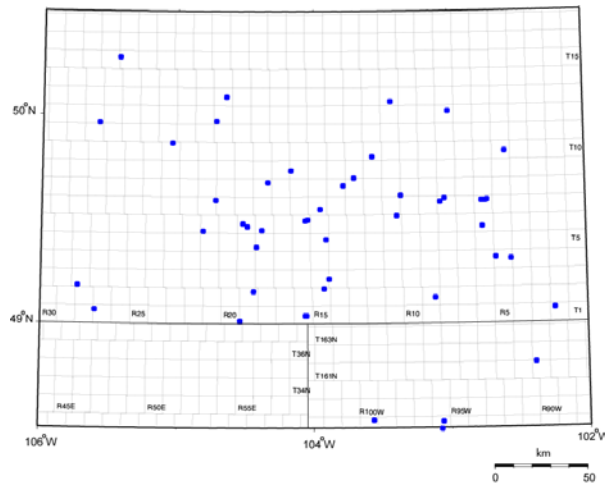


Figure 1. Study area including SE Saskatchewan, Canada, NE Montana, and NW North Dakota, U.S.A. DST data distribution provides reasonably good coverage for building a geostatistical model of permeability.

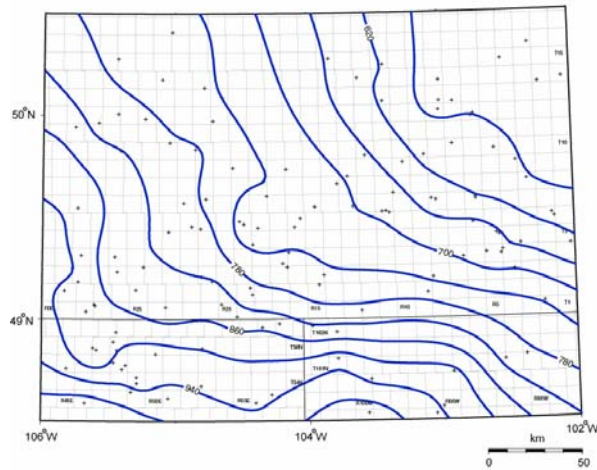


Figure 2. Potentiometric surface of the Birdbear aquifer constructed from extrapolated DST pressure measurements

## Background

The geostatistical simulation approach to modeling geological heterogeneity is based on modeling two-point correlations between rock properties at different locations in a domain. These correlations are calculated via the experimental semivariogram, which is the basis for a structural model of spatial variability of the sampled petrophysical property [7]. This structural model is then used to estimate at unsampled locations with kriging, which computes a statistically unbiased, best-fit estimate at each node accounting for the hard data values as well as the correlation between the data. Stochastic simulation then corrects for the artificially smooth result of kriging, reproducing the full variability, or heterogeneity in the property being modeled.

## Methodology

Prior to calculating semivariograms and kriging, data should be declustered for representative statistics. If it is possible to determine a secondary variable correlated to effective permeability, sampling bias may be corrected as well. For details on declustering and debiasing, the reader is referred to Deutsch [4]. The histogram of Birdbear DST data (Figure 3) was not improved by declustering, and sample bias as a result of preferentially drill-stem testing higher porosity zones was intractable. Had some systematic bias been detected in the comparison of any given well log response over the DST interval versus the log response over the entire formation, sampling bias could have been corrected to some degree.

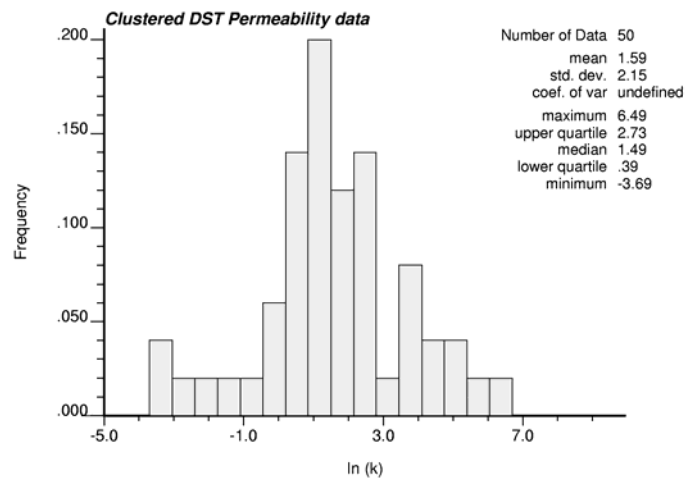


Figure 3. Histogram of natural log of permeability calculated from Birdbear DST data.

### *Variography*

The methodology employed in this study assumes a Gaussian random function model [3] for permeability. If there is prior information suggesting the need to model connected extreme values in the permeability distribution, such as high permeability channel sands, an indicator formalism should be used. In this case, there was no such prior knowledge. As such, the permeability data were transformed to a standard normal distribution prior to calculating semivariograms and kriging.

A variogram map and experimental semivariogram of the DST data is shown in Figure 4. The anisotropy is clear with the direction of maximum continuity (i.e., shallowest increase in the variability) oriented at approximately 130°. Care should be taken in selecting parameters for variogram calculation that capture legitimate structures in the data rather than data artifacts. The cyclicity in the direction of minimum continuity, at an azimuth of 40°, was confirmed by adjustment of the lag distance in the semivariogram calculation to ensure the period of the observed cyclicity did not shift. A hand-contoured map of the data also revealed alternating areas of high and low permeability data. Other notable features in the experimental semivariogram are a trend in the direction of maximum continuity, with the variability rising above the global variance and an associated zonal anisotropy in the direction of minimum continuity, expressed as a sill below the full variance in the data.

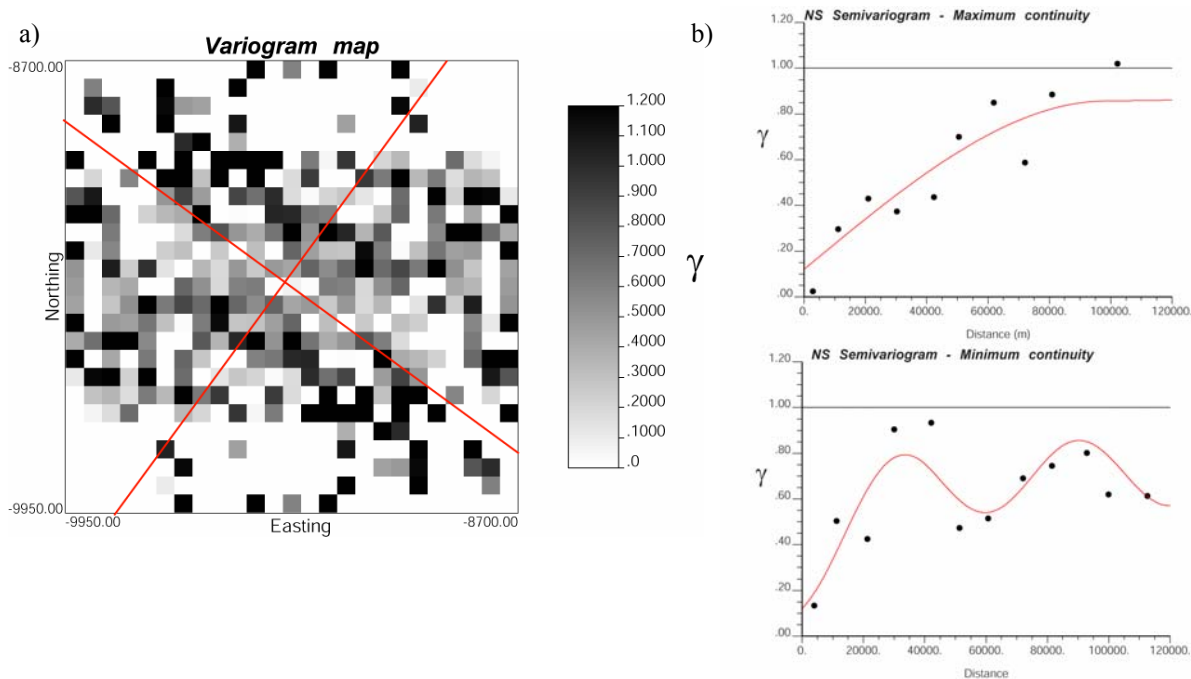


Figure 4. a) Variogram map of Birdbear DST data with principal directions of anisotropy. Maximum spatial continuity direction oriented at approximately 130°. b) Experimental semivariograms shown as points, and anisotropic variogram model overlain as solid lines.

### *Kriging and the probabilistic model*

Variogram models are fit to the experimental semivariograms under certain constraints to ensure a valid covariance model (Figure 4). The variogram model enforces the correct covariance between the data as a function of distance and direction. Kriging provides an unbiased optimal solution to the problem of estimating at unknown locations. The best fit to the data is artificially smooth (Figure 5). The kriged estimates do not produce a good map of permeability as inferred from inter-well variability because variability between the estimated locations is not honoured.

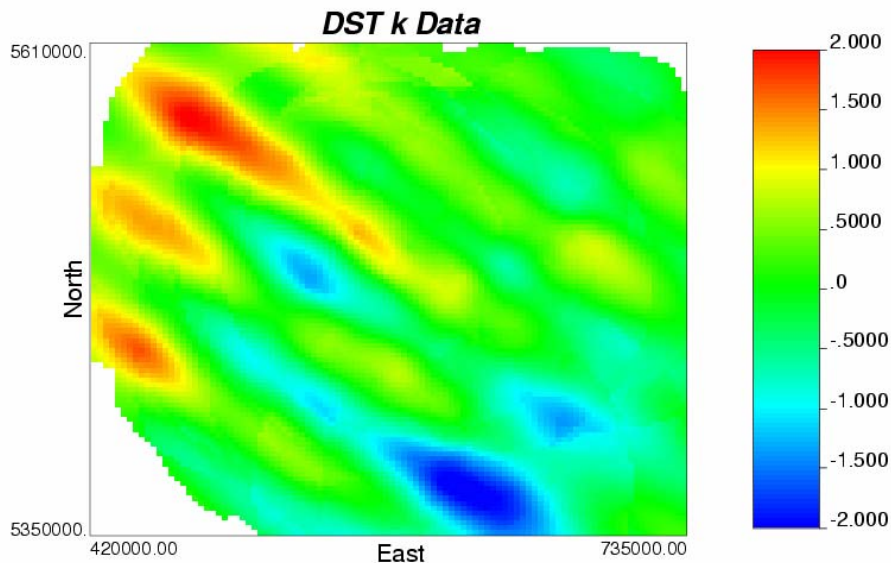


Figure 5. Kriged Birdbear DST permeabilities. Colour scale shows normal score transformed values with mean of 0.0 and variance of 1.0.

Despite the fact that the kriging results are not particularly useful on a contour plot, they provide the essential information about the conditional probability model. At each node, there is a conditionally unbiased, best-fit estimate and an associated estimation variance quantifying the local uncertainty in that estimate. This information can be used to validate the probability model. A cross plot of estimates versus the true values at data locations in a “leave-one-out” cross-validation routine reveals the predictive ability of the model (Figure 6a). A plot of errors versus true values should show no systematic bias about the zero-error line if the model is indeed conditionally unbiased (Figure 6b). An accuracy plot [4], another “goodness” test, can also assess the accuracy and precision of the model.

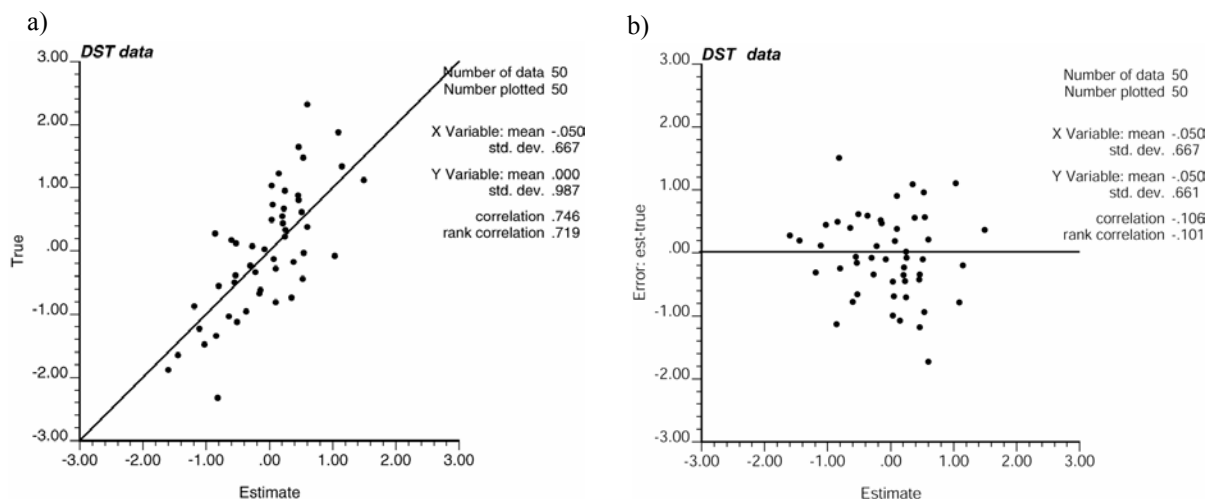


Figure 6. a) True value versus estimated value at the same location when the datum is removed. The correlation coefficient of 0.75 indicates good predictive ability of the probability model. b) Cross plot of error (estimated value – true value at that location) versus the estimate in a leave-one-out cross validation of the probability model. Even spread around the 1:1 bisector indicates no conditional bias.

### Stochastic Simulation

Stochastic simulation reproduces the variability in the permeability estimates that is inherent to the data. The essence of simulation is the addition of a randomly drawn residual to the kriged estimate to correct for the smoothing effect of kriging. The residual is obtained by Monte Carlo simulation from the local conditional distribution that defines the uncertainty in the estimate at that node. Simulation thereby reproduces the joint spatial variability between the data, the data and the estimates, and the estimates themselves. Figure 7 shows a set of equally probable realizations of Birdbear permeability generated by Sequential Gaussian Simulation using SGSIM [3].

### Variogram scaling

The permeability data have an intrinsic variance related to the sample support volume (the scale of the data), which necessarily decreases as the data are made to inform larger volumes. A Birdbear DST may have a radius of investigation of 15–25 m, so scaling of the histogram and

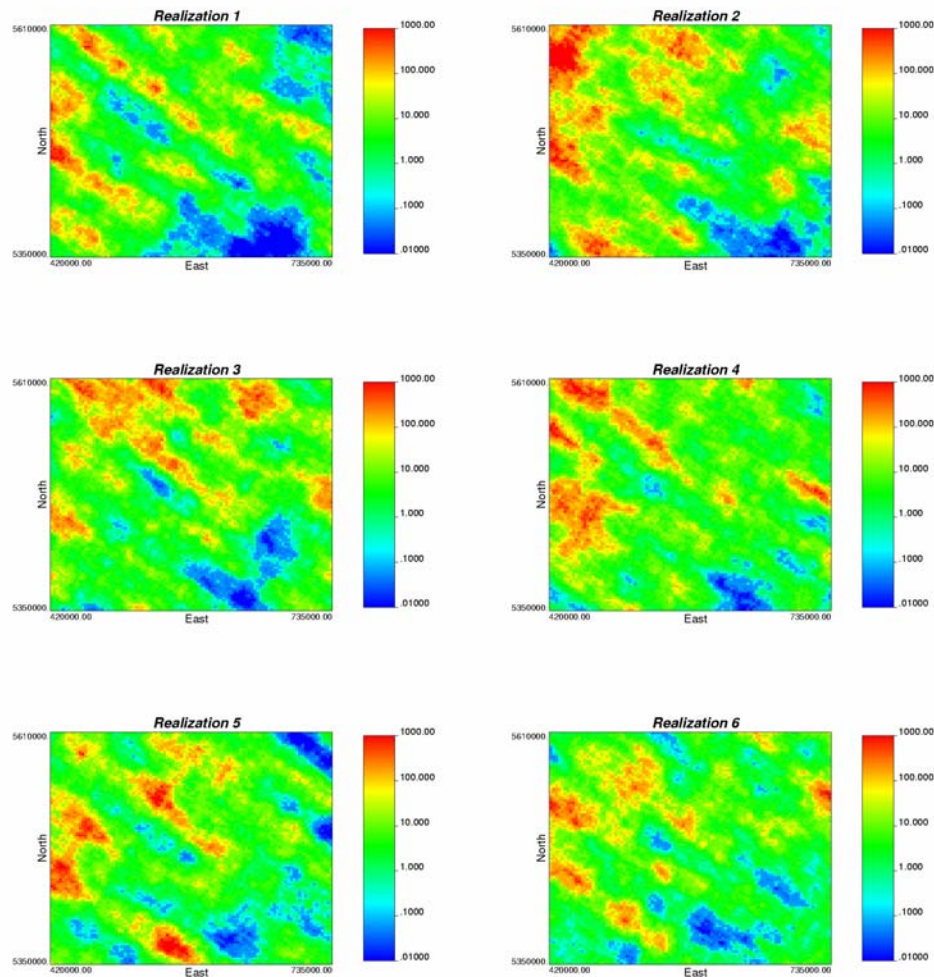


Figure 7. Equally likely realizations of Birdbear permeability consistently reproducing the data and the variogram model. Colour scale shows log permeability in millidarcies.

variogram [8,9] is necessary to get the correct variance at the grid scale (cells of 3150 x 2600 m). The upscaled variogram models have an extended range and a decreased nugget effect, as short scale variability in the permeability data cannot be resolved at regional mapping scales (Figure 8). The reduction in variance is clear in the simulation results (Figure 9). Because Sequential Gaussian Simulation estimates in standard Gaussian space, the global variance should be 1.0. Simulation is thus performed by renormalizing the variance contributions of the scaled variogram model back to a sum of 1.0, and applying the scaled histogram as a reference distribution to account for the dispersion variance.

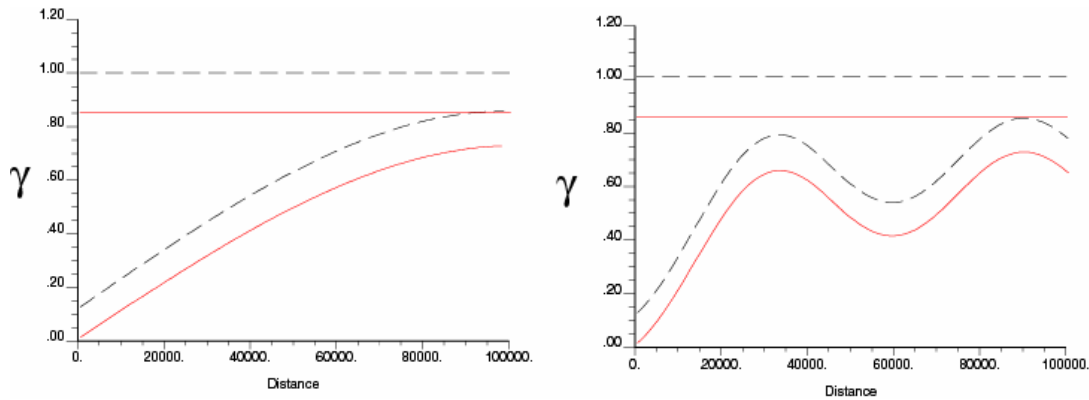


Figure 8. Scaled DST variogram model (solid lines). The effect of considering the data to inform a block size larger than their original support scale is a global reduction in variability (reduced sill from 1.0 to 0.86) and a reduced nugget effect.

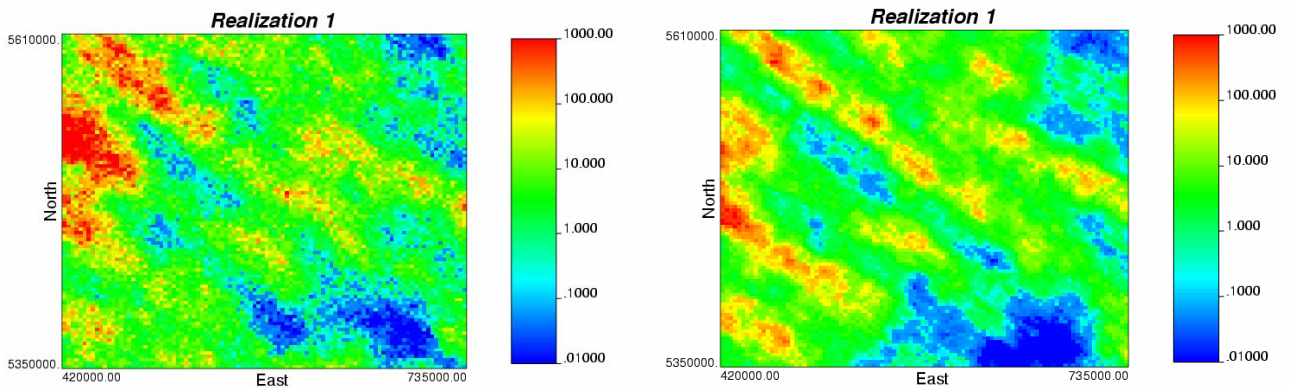


Figure 9. One realization generated with the original variogram model (left) compared to the same realization generated using the scaled histogram and variogram model. The decreased nugget effect results in a smoother map as short scale data variability cannot be resolved at the simulation scale.

### *Post-processing realizations*

A probabilistic approach to the problem of generating images of geologic heterogeneity is necessary given the degree of uncertainty in the true permeability distribution and in the data

themselves. The result of conditional stochastic simulation is a number of equally probable realizations of the permeability distribution, each of which honours the measured data at the data locations. The multiple realizations give a set of statistically equivalent models by which uncertainty can be quantified; however, a given realization should reproduce the observed hydraulic head distribution to be physically meaningful. Merging the geostatistical approach with a sequential self-calibration (SSC) algorithm [6] for inversion of the observed hydraulic heads is one way to obtain physically meaningful realizations of permeability, however such a complex approach will rarely be used in practice. Alternatively, a simple exclusion criterion is to reject any realization whose corresponding flow solution is greater than a minimum threshold value for average error between the simulated and reference head field.

It is, in any case, necessary to run steady state flow simulations with the generated permeability distributions to verify reasonable reproduction of the potentiometric surface. This qualitative check is indispensable since most of the anomalies in the potentiometric surface can be related directly to the distribution of permeability. For the Birdbear aquifer study, steady-state flow simulations were run using a set of 100 permeability realizations. The boundary nodes from a kriged hydraulic head grid were used as constrained head values for the flow simulations. Flow simulations were set up to loop over the realizations and the solutions compared to the reference potentiometric surface by their Root Mean Squared error. One run was performed with a homogenous permeability field to ensure that the flow solutions were not governed more by the boundary conditions than by the permeability distributions. Figure 10 depicts two selected realizations and their corresponding modeled hydraulic head fields.

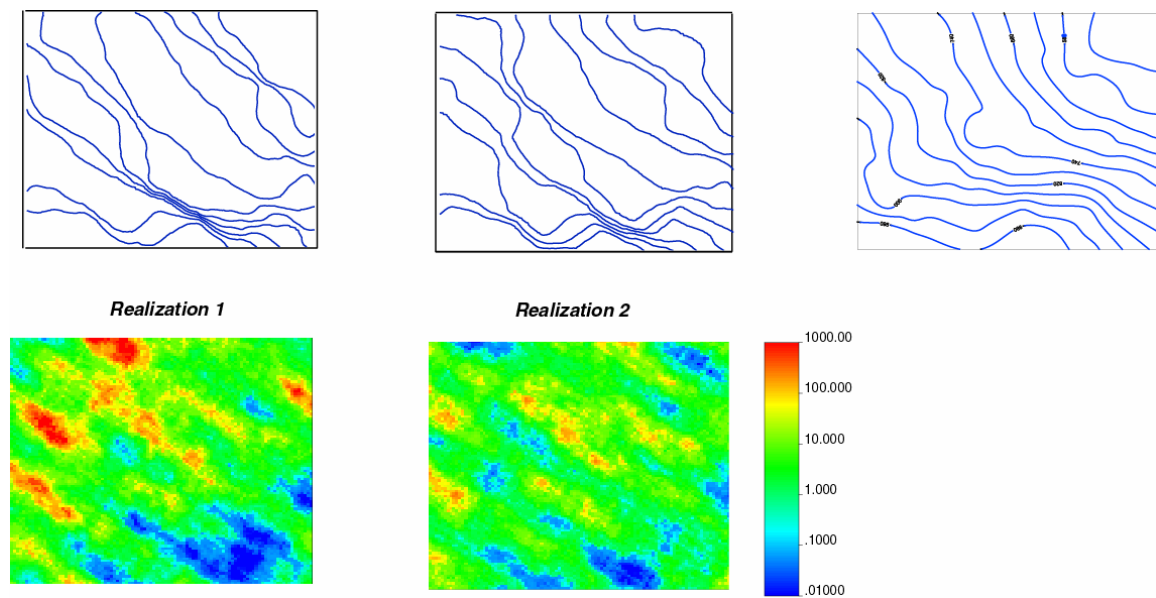


Figure 10. Steady state flow simulations for two realizations of Birdbear DST permeability distributions with the reference potentiometric surface map shown at far right.

The flow simulations should reproduce features of the potentiometric surface map and the closeness of the reproduction of these features reflects the accuracy of the permeability realizations. Better matches than those obtained would require that the data better inform the spatial structure of the heterogeneity. Stochastic simulation will rarely produce a near-perfect

match to the observed hydraulic heads since the flow physics are not taken into account, however its simplicity will often outweigh the added benefits of more complex methods such as SSC, if such an approach would be considered at all.

In the absence of specified fluxes, the steady-state flow solutions will not reflect the absolute permeability magnitudes, but only the relative contrasts between adjacent grid block permeabilities. A comparison of the average total throughflow of the flow simulations to the estimated steady state flow across the map area will suggest whether the permeability magnitudes are realistic. Once a set of deemed-representative realizations is selected, groundwater fluxes may be calculated using Darcy's law. Darcy's Law may be stated most simply as:

$$q = -Ki$$

where  $q$  is the groundwater flux (specific discharge),  $K$  is hydraulic conductivity, and  $i$  is the gradient of hydraulic head. The magnitude of hydraulic gradient,  $i$ , may be calculated at each node and multiplied by the hydraulic conductivity. The conversion of permeability to hydraulic conductivity is rudimentary. Figure 11 shows the resultant groundwater fluxes calculated from a selected permeability realization for the Birdbear Aquifer and the resultant distribution of fluxes over the domain.

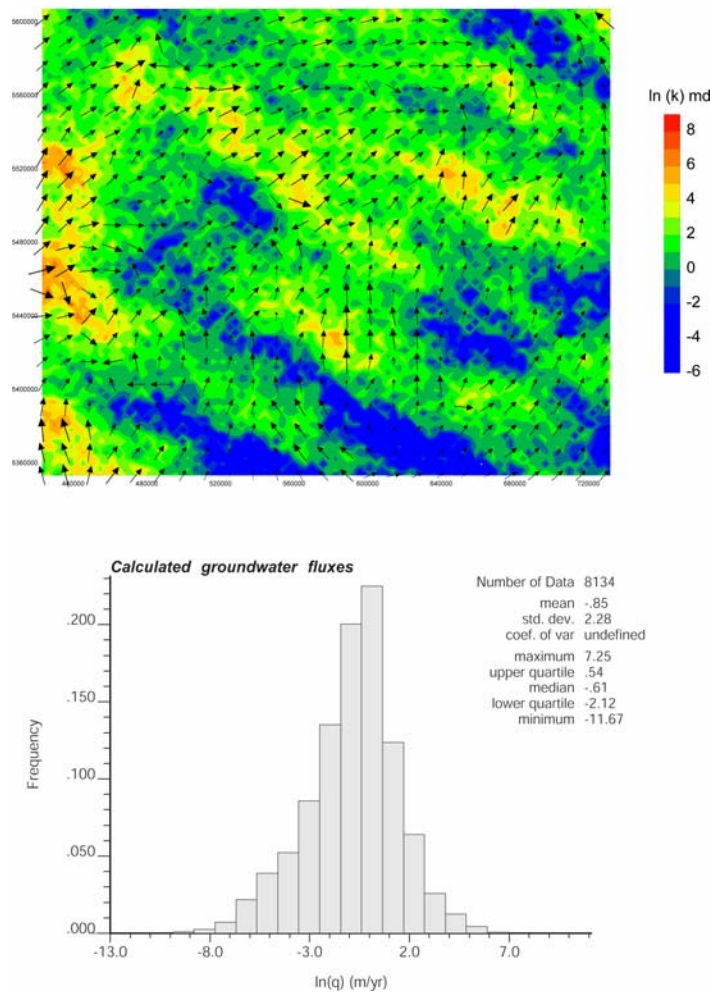


Figure 12. Calculated groundwater flux vectors based on observed hydraulic gradients and a selected permeability realization. The range of flux magnitudes is shown in the histogram at bottom.

## Summary

Classical variography, estimation, and simulation can be combined into a practical methodology to create maps of regional permeability to complement hydrogeological mapping studies. A geostatistical simulation approach does not give a single best answer; rather, it accounts for and makes use of the uncertainty in the data via multiple realizations. Post processing multiple permeability realizations generated by stochastic simulation may enable the selection of one or more realizations as adequately representative “maps” of permeability. An exclusion criterion, such as the smallest average error between modeled and observed heads for a set of flow simulations, can be used to select a best-fit realization from a set of equiprobable realizations of permeability. Once a small number of realizations, or even one best realization is selected as representative of the permeability field, spatially variable groundwater fluxes over the map area may be estimated.

## References

- [1] Alkalali, A., 2002, Petroleum Hydrogeology of the Nisku Aquifer: M.Sc. thesis, Alberta, Edmonton, 152 p.
- [2] DeMis, W. D., 1995, Effect of cross-basinal hydrodynamic flow on oil accumulations and oil migration history of the Bakken-Madison petroleum system Williston Basin, North America: Seventh International Williston Basin Symposium, p. 291-301.
- [3] Deutsch, C. V., and A. G. Journel, 1997, GSLIB, Geostatistical Software Library and Users Guide: New York, Oxford, Oxford University Press, 369 p.
- [4] Deutsch, C. V., 2002, Geostatistical Reservoir Modeling, Oxford University Press, 384 p.
- [5] Downey, J. S., J. F. Busby, and G. A. Dinwiddie, 1987, Regional aquifers and petroleum in the Williston Basin region of the United States: 1987 Symposium of the Rocky Mountain Association of Geologists, p. 299-312.
- [6] Gomez-Hernandez, J. J., A. Sahuquillo, and J. E. Capilla, 1997, Stochastic simulation of transmissivity fields conditional to both transmissivity and piezometric data 2. Demonstration on a synthetic aquifer: Journal of Hydrology, v. 203, p. 175-188.
- [7] Journel, A. G., and C. J. Huijbregts, 1978, Mining Geostatistics: London, Academic Press, 600 p.
- [8] Kupfersberger, H., C. V. Deutsch, and A. G. Journel, 1998, Deriving Constraints on Small-Scale Variograms due to Variograms of Large-Scale Data: Mathematical Geology, v. 30, p. 837-852.
- [9] Oz, B., C. V. Deutsch, and P. Frykman, 2002, A visualbasic program for histogram and variogram scaling: Computers & Geosciences, v. 28, p. 21-31.
- [10] Tóth, J., and K. Rakhit, 1988, Exploration for reservoir quality rock bodies by mapping and simulation of potentiometric surface anomalies: Bulletin of Canadian Petroleum Geology, v. 36, p. 362-378.